# A Comparison of Uranium Oxide and Nickel as Single-layer Reflectors from 2.7 to 11.6 Nanometers

Richard L. Sandberg, David D. Allred*, Jed E. Johnson, R. Steven Turley
Department of Physics and Astronomy, Brigham Young University,
N-283 ESC, Provo, UT USA 84602

## ABSTRACT

We present the measured reflectances (Beamline 6.3.2, ALS at LBNL) of naturally oxidized uranium and naturally oxidized nickel thin films from 2.7 to 11.6 nm at 5°, 10°, and 15° grazing incidence. These show that uranium, as $UO_2$, can fulfill its promise as the highest known single surface reflector for this portion of the soft x-ray region, being nearly twice as reflective as nickel in the 5-10 nm region. This is due to its large index of refraction coupled with low absorption. Nickel is commonly used in soft x-ray applications in astronomy and synchrotrons. (Its reflectance at 10° exceeds that of Au and Ir for most of this range.) We prepared uranium and nickel thin films via DC-magnetron sputtering of a depleted U target and resistive heating evaporation respectively. Ambient oxidation quickly brought the U sample to $UO_2$ (total thickness about 30 nm). The nickel sample (50 nm) also acquired a thin native oxide coating (<2nm). Though the density of U in $UO_2$ is only half of the metal, its reflectance is high and it is relatively stable against further changes. There are important discrepancies between $UO_2$'s actual reflectance with those predicted by the atomic scattering factor model indicative of the need to determine the actual constants of $UO_2$.

**Keywords:** soft x-ray, EUV, low-angle reflector, nickel, uranium oxide, synchrotron, EUV/soft X-ray astronomy

## 1. INTRODUCTION

### 1.1 Uranium as a soft x-ray reflector

This article reports the most recent results in our group's investigation of the possibility that uranium thin films can be used to increase the low-angle reflectance currently available for thin-film single-layer reflectors at about 5-9 nm.[1] Here we report on recent reflectance measurements from 2.7 to 11.6 nanometers comparing naturally oxidized uranium to nickel (and nickel oxide) thin-film reflectors. Nickel was chosen for the reflectance comparison because of its wide use as a thin-film reflective coating in optical systems for the EUV and soft x-ray range.[2] Nickel's average reflectance exceeds that of gold and iridium, the other common choices for reflectors in this range. The uranium oxide and nickel samples were deposited through DC magnetron sputtering and thermal evaporation respectively at Brigham Young University. The reflectance measurements were conducted at the Advanced Light Source's Beamline 6.3.2 at the Lawrence Berkley National Laboratory. Additional measurements were made with a VUV monochromator with helium hollow-cathode source at BYU. We find that the low-angle reflectance of uranium oxide surfaces exceeds that of nickel over a large wavelength range.

As noted elsewhere, the optical properties of uranium are noteworthy over much of the EUV[3] and soft x-ray[1] portions of the spectrum. Uranium metal is very dense (bulk density about 19 g/cm$^3$). It has 92 electrons that may interact with photons over many energy ranges. One of the unique properties of uranium is that over a relatively large range around 6 nm (200 eV) it has a very large index of refraction coupled with very modest absorption. The $\delta$ - $\beta$ scatter plot (Fig. 1) for various elements at 4.47 nm (277 eV) shows that no other element has a $\delta$ as high, and its $\beta$ is remarkable low. The reported beta of uranium is less than one-quarter of Ni and other 3d elements and less than one-sixth the value of Ir and other 5d elements. The question has been, in light of uranium metal's susceptibility to oxidation, whether its promise can be realized. We show here that it can be.

*allred@byu.edu; phone 1 801 422-3489; fax 1 801 422-0553; http://xuv.byu.edu



Advances in Mirror Technology for X-Ray, EUV Lithography, Laser, and Other Applications,
edited by Ali M. Khounsary, Udo Dinger, Kazuya Ota, Proceedings of SPIE Vol. 5193
(SPIE, Bellingham, WA, 2004) · 0277-786X/04/$15 · doi: 10.1117/12.523478

Downloaded From: http://proceedings.spiedigitallibrary.org/ on 03/19/2014 Terms of Use: http://spiedl.org/terms

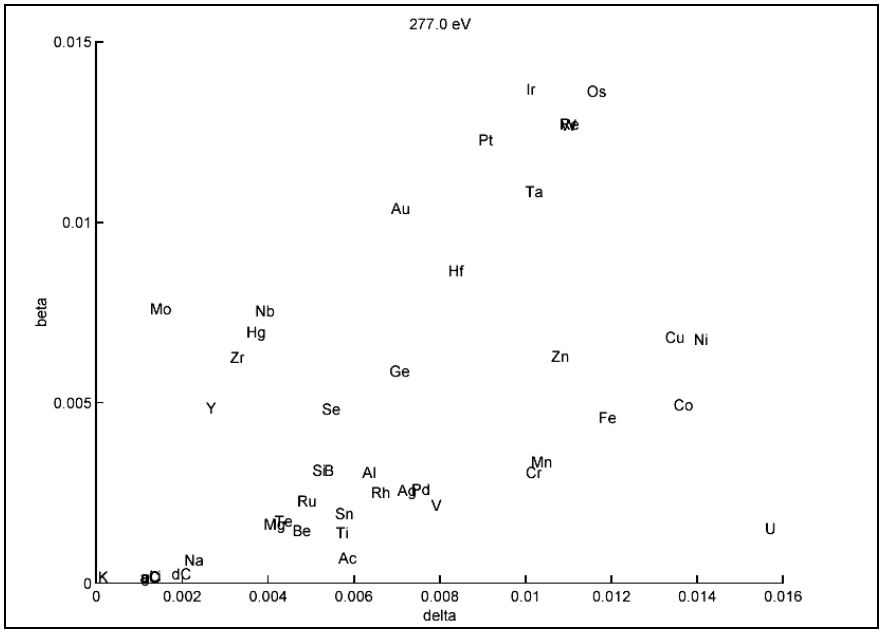



**Fig. 1: The δ - β plot for several elements at 4.48 nm (277 eV). Nickel and its neighboring 3d elements are the nearest to uranium in this area.[4]**

There have been several efforts to use uranium and, later, its oxides, as constituents in reflectors.

1. A group at MOXTEK investigated the preparation of U/Sc multilayer mirrors in the water window in 1993-5. This approach relies on the low absorption of uranium to allow many layers in a multilayer to participate in multilayer reflectivity and uses the high delta to produce high amplitude reflectance at each interface.[4]
2. Our group used uranium in the late 1990's to prepare several near-normal-incidence U/Si EUV mirrors with high reflectance at 30.2 nm (41 eV) and low reflectance at 59.0 nm (21 eV)[3] for the Image spacecraft which currently orbits the Earth.[5] It should be noted that the design incorporated the fact that the top uranium layer is oxidized. This was our first realization that the native oxide which forms on uranium might be useful in its own right in optics.
3. A third potential application of uranium for broadband, low-angle-of-incidence mirrors for the 4.1 to 12.4 nm (100 to 300 eV) range was suggest to us by Prof. Webster Cash (University of Colorado).[2] He had performed calculations in the mid 1990s indicating that uranium might produce phenomenal single-surface mirrors for x-ray astronomy, perhaps twice as reflecting as the nickel, gold or iridium mirror traditionally used for low-angle reflectance. We reported our first soft x-ray measurements of uranium films with and without an ultra thin carbon "barrier" top layer a year ago at this meeting.[1]

This paper reports follow up research on this earlier work. We compare the soft x-ray, low-angle reflectance of uranium covered with its native oxide ($UO_2$)[6] to nickel, a standard material for low-angle, soft x-ray reflectance. The nickel also has a native oxide, NiO, but, for the same exposure to air, it is much thinner than the $UO_2$; although, NiO like Ni is very absorbing.

### 1.2 In principle, U is more reflective than Ni

We used the CXRO's (Center for X-ray Optics) website to compute the reflectance for uranium, uranium oxide, nickel, and nickel oxide at 5˚ grazing incidence angle (see Fig. 2).[7] From this figure we can see the expected value of uranium as a EUV/soft x-ray reflector because its reflectance nearly doubles that of nickel. Note that since these curves are computed, actual thin films could be expected to show somewhat different reflectance. This is because the surfaces of the films may have some roughness and because their densities and compositions might differ from bulk.



Downloaded From: http://proceedings.spiedigitallibrary.org/ on 03/19/2014 Terms of Use: http://spiedl.org/terms

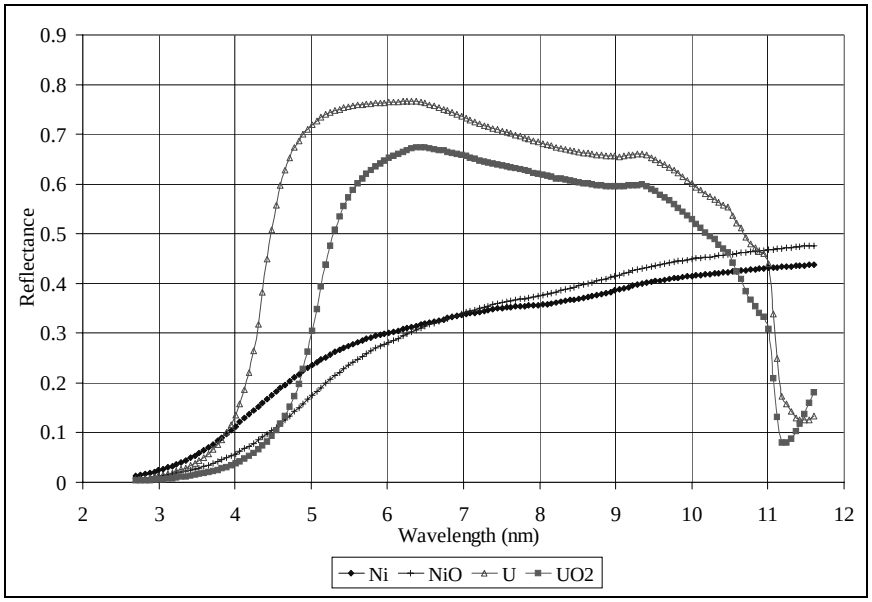



**Fig. 2: The reflectance at 5˚ from grazing for Ni, NiO, U, and UO2 predicted by the atomic scattering factor model from the CXRO website.[6]**

## 2. METHODOLOGY

### 2.1 Sample preparation/experimental setup

The uranium oxide and nickel samples were deposited on pieces of commercially available, polished silicon test wafers (100 orientation). The typical surface roughness was examined using AFM and was ~0.02 nm over a 100 by 100 nm area. The DC magnetron sputtering and evaporation systems are located in the Department of Physics and Astronomy at Brigham Young University and the processes followed are similar as those described in previous works by the BYU EUV group.[1,3,5,6,8] Below we include brief reviews of significant information of the deposition process.

### 2.1.1 $UO_2$ deposition through DC magnetron sputtering

We used a DC magnetron sputtering system on the Brigham Young University campus to deposit the uranium sample.[8,9] The materials to be sputtered are made into targets which are fastened onto the top of the sputter guns. Using a roughing pump, we evacuated the chamber to a pressure of about 100 mtorr. At this point, the pump is switched by opening a large gate valve to a cryopump (CryoTorr 8) which then evacuates the system down to a base pressure of $4.5*10^{-6}$ torr. An ion gauge reads the base pressure of the system. The cryopump is then shuttered to allow the pressure of the chamber to rise to the working pressure for a limited amount of argon gas. An Edwards Model 655 Barocel® capacitance manometer reads the working pressure of the system. This capacitance manometer is a 100-millitorr full-scale vacuum/pressure transducer. Furthermore, a Ferran Scientific Multipole (quadrapole mass) Analyzer (MPA) was used to read the total pressure and the partial pressures of gas species present. Then 99.999% pure argon gas is introduced into the chamber through mass flow controller. When the chamber pressure due to the introduced argon reaches a pressure of about of 3 mtorr, as measured on the MPA, a large DC negative voltage is placed on the sputtering guns. The voltage ionizes the argon, creating argon plasma which impacts with the negatively charged target atop the gun. This impact removes uranium atoms which then deposit on the sample held upside down above the sputtering targets. The uranium sputter targets used here were of depleted uranium metal (less than 0.2% U-235). Thus the decay per second of depleted uranium is about 0.238 alphas, twice as many betas and miscellaneous L x-rays for each $cm^2$ of a 10 nm film at bulk density. The users' solid angle of detection of these will be considerably less than 2 pi steradians.



Downloaded From: http://proceedings.spiedigitallibrary.org/ on 03/19/2014 Terms of Use: http://spiedl.org/terms

(Half go down into the substrate and are absorbed.) So counts from the mirror will be small compared to background for soft x-ray applications.

The target thickness for our sample after oxidation was 30 nm as measured by XRD. (A uranium film oxidizing completely to $UO_2$ is calculated, based on handbook densities, to double in thickness, so the initial films were thinner.)[10] Deposition rates were determined by using XRD to get the periods of several different multilayers containing the desired materials and are described previously.[8] After sputtering, the uranium was allowed to oxidize naturally in laboratory air since its removal from the vacuum chamber 63 days before measuring thickness. Prior to this study, studies of the oxidation rates of uranium thin films have been conducted.[6] Uranium is subject to extensive oxidation in laboratory air, about 6 nm in 13 min, and more than 13 nm in a day. Oliphant further showed that the uranium oxidizes into films of $UO_{2+x}$ (x~0) which can be a few nanometers thick under typical laboratory conditions (room ambient). It should be noted that many bulk oxides of uranium are known. Even for a given composition, such as $UO_3$, many different crystal structures are known. Also $UO_2$ tolerates a large range of nonstoichiometry. The value of x in $UO_{2+x}$ can reach 0.25 before inducing crystal changes. Members of our group are currently studying these subtleties using XPS and TEM.[11,12] For the purpose of this paper the oxide will be called $UO_x$; although, it is closest to $UO_2$ whose stoichiometry and handbook density of 10.59 g/cm$^3$ will be used in calculation in accordance with Oliphant's findings.[6] When we refer to the reflectance and other properties of the uranium oxide film used in the study, it should be understood that this means the most abundant natural oxide of uranium, $UO_2$.

### 2.1.2 Ni deposition through thermal evaporation

Our nickel films were prepared by evaporating Ni wire from a resistively heated tungsten boat (RD Mathis Co.) in a large, cryopumped, stainless steel "bell jar" coater. The base pressure of the system was 3.2 x10$^{-4}$ Pa (2.4 x10$^{-6}$ torr). A quartz crystal monitor was used to measure the evaporation rate. The source was shuttered as the voltage to the tungsten boat was increased. When the evaporation rate reached about 1-2 nm/s, the shutter was opened and the substrates were coated. Fast deposition rates are known to be preferable in obtaining the highest reflectance for aluminum and many materials. This is probably due to their limiting the extent to which impurities, usually oxygen, are drawn into the film from residual air and water vapor in the vacuum. After the monitor recorded about 91 nm of film the voltage to the source was cut, the box was vented to air and the films removed for further study. They were allowed to naturally oxidize for two days before XRD thickness measurement and ten days before measurement at the Advanced Light Source.

At the time the films were deposited, the tooling factor of the crystal monitor for the position of the substrates was not known. After the thickness of the film on Si was determined via XRD (see below) to be about 50 nm the tooling factor of the crystal monitor was seen to be about 55%. The crystal monitor was set significantly closer to the evaporation boat than the substrates, though to one side. So this tooling factor is consistent with geometry. Since the surface roughness of crystalline materials usually increases with increasing film thickness and surface roughness decreases reflectance, we wanted thinner Ni films. Calculations had indicated that all Ni films thicker than about 30 nm should have the same low-angle, soft x-ray reflectance over our range of interest. The target thickness for the nickel film was chosen as between 30 and 60 nm.

### 2.2 Thickness determination: Characterization with XRD and IMD Fitting.

Thin-film interference of x rays was used to determine the thickness of our deposited thin films. Using a Scintag® X-ray diffractometer (XRD), we measured the low-angle reflectance maxima and minima. The Scintag diffractometer produces collimated x ray radiation from a rotating copper target, which was scattered off of the sample. A liquid nitrogen cooled intrinsic germanium detector in photon counting mode was gated to accept $K_\alpha$ radiation (0.154 nm) and reject $K_\beta$ and bremstrahlung radiation above and below Cu $K_\alpha$. Angle scans at low angles (usually from 1-3.5˚, 2θ, grazing incidence angles) were taken. These scans showed interference fringes. At first-order approximation, the data can be modeled with an equation which resembles the Bragg diffraction, $m\lambda=2d\sin\theta$, where $m$ is the diffraction order, λ is the wavelength of the diffractometer radiation in the material being measured, $d$ is the layer thickness, and $\theta$ is the angle between the incident and refracted beam.[8] The Bragg equation as written above does not take into account the refraction of the x rays in the material. It is adequate for approximating the thickness of the film but to properly obtain



Downloaded From: http://proceedings.spiedigitallibrary.org/ on 03/19/2014 Terms of Use: http://spiedl.org/terms

the thickness we must match the spectra with a computer model. We used IMD to model our layers.[13] Then by adjusting the thickness of the modeled layer, the diffraction peaks of the model and the measured XRD scan can be compared until the numbers of peaks in the same angle interval are the same and the peak positions match. The computed value for thickness is then approximately the same as the real layer thickness. For nickel, this thickness was 49.7±0.5 nm. For the uranium oxide sample this was 31.8±0.5 nm.

The transmission of the nickel film on quartz and the ellipsometric constants for the nickel film on silicon were also measured using a John A. Woollam Company M2000D model spectroscopic ellipsometer with rotating compensator for the interval 189 to 1000 nm. The transmission and the ellipsometric data were concatenated and modeled using standard software. At ~50 nm the Ni film was still sufficiently transparent in transmission to constrain the thickness of the nickel as finite. Fixing the thickness to that given by XRD gave a low MSE, mean square error. The indices of NiO were not known, but the model could still constrain the thickness of the native oxide which forms on our Ni films in a period of a few days to less than 2 nm and probably greater than 1 nm.

### 2.3 ALS Reflectometry

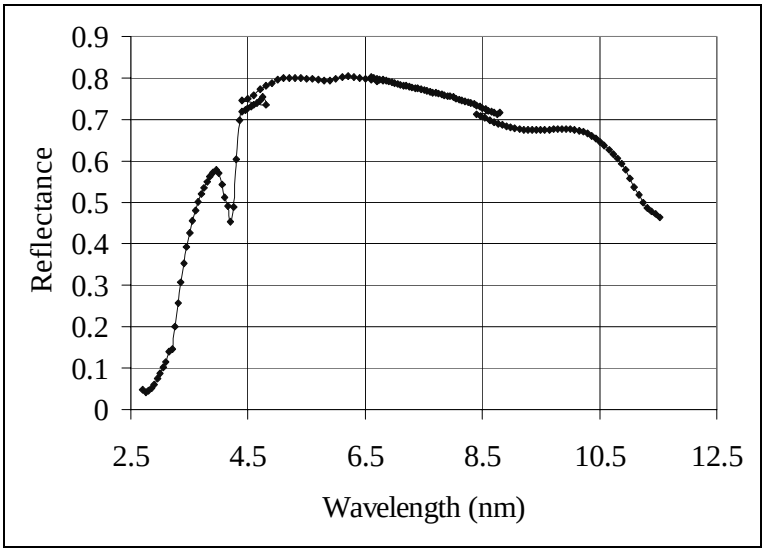



**Fig. 3: Measured reflectance of $UO_x$ from ALS Beamline 6.3.2 at 5˚. Notice the slight discrepancies in the reflectance caused by the use of different filters over different wavelength regions which do not suppress extraneous orders.**

The reflectance measurements were conducted at the Advanced Light Source (ALS) at Lawrence Berkley National Laboratory at the University of California-Berkley on Beamline 6.3.2. This beamline has a reflectometer setup with three gratings (200 lines/mm, 600 lines/mm, and 1200 lines/mm) which allow the user to measure sample reflectance from 1 to 24.8 nm (50 to 1300 eV) at various angles.[14] Different filters corresponding to these gratings select which wavelength ranges are desired. However, the filters do not perfectly suppress other orders than the desired order, so the source is not perfectly monochromatic. This non-monochromatic nature can cause measured reflectances of overlapping wavelength regions to differ slightly as can be seen in Fig. 3 at 4.5, 6.6, and 8.5 nm. Reflectances can also vary from range to range if the beam strikes a different part of the sample. Some of the measurements on the nickel samples were made after the sample had been removed and then returned to the reflectometer. We attribute the inconsistencies seen in our measured data (section 3) to these two factors. For each wavelength scan, an $I_0$ scan (beam intensity) was taken by removing the sample and then taking data of only the source beam. Additionally, background noise scans were taken by completely blocking the source and colleting data of the background noise. The process of normalization to extract reflectances are described in more detail along with further details on Beamline 6.3.2 at the CXRO webpage and can be found in Underwood.[7,14,15]



Downloaded From: http://proceedings.spiedigitallibrary.org/ on 03/19/2014 Terms of Use: http://spiedl.org/terms

### 2.4 Modeling reflectances

The reflectance of light from an abrupt surface can be calculated when the indices of refraction are known. This is true whether the surface is a bulk material or composed of many thin distinct layers as long as the thicknesses, diffusion between layers, surface roughness, material density, and indices of refraction of each material are known.

While the values of the structure characteristics mentioned above change with wavelength, this algorithm can still be followed in the EUV range as well as in the visible. There is one important difference for the EUV and x-ray ranges. In the visible, it is understood that someone must have measured the indices of refraction of each of the materials before the reflectance can be calculated. However, at lower wavelengths (EUV and x ray), it is assumed that having measured the optical constants of the individual elements composing the materials is sufficient.

Here we quote from the CXRO webpage:

> The primary interaction of low-energy x rays within matter, viz. photoabsorption and coherent scattering, have been described for photon energies outside the absorption threshold regions by using atomic scattering factors, $f = f_1 + if_2$. The atomic *photoabsorption cross section*, $\mu_a$, may be readily obtained from the values of $f_2$ using the relation:
>
> $$\mu_a = 2 \cdot r_0 \cdot \lambda \cdot f_2$$
>
> where $r_0$ is the classical electron radius, and $\lambda$ is the wavelength. The transmission of x rays through a slab of thickness $d$ is then given by:
>
> $$T = \exp(-n \cdot \mu_a \cdot d)$$
>
> where $n$ is the number of atoms per unit volume in the slab. The *index of refraction* $\tilde{n}_r$ for a material is calculated by:
>
> $$\tilde{n}_r = \frac{1 - n \cdot r_0 \cdot \lambda \cdot (f_1 + if_2)}{2\pi}$$
>
> These (semi-empirical) atomic scattering factors are based upon photoabsorption measurements of elements in their elemental state. The basic assumption is that condensed matter may be modeled as a collection of non-interacting atoms. This assumption is in general a good one for energies sufficiently far from absorption thresholds. In the threshold regions, the specific chemical state is important and direct experimental measurements must be made.[16,17]

Several problems arise with the standard atomic scattering factor model (ASF). First, if the atomic scattering factors are not well measured, as is the case with uranium in the region being discussed, then accurate reflectances cannot be calculated. Additionally, the model does not include effective chemical bonds. As stated by Gullikson and Henke above, near absorption regions these aspects become increasingly important. This is the case with our study of uranium because of the predicted absorption edge in uranium near 11.1 nm. As will be discussed later, several discrepancies arise between the measured and calculated reflectance of uranium leading us to conclude that a more thorough measurement of uranium's indices of refraction is necessary.

For this study, we used two computer programs to calculate reflectance: the CXRO website and IMD.[7,13] Neither of the programs contains measured uranium oxide optical constants. Instead both ask for data. The CXRO web site uses the ASF approach as described above. The user gives it the chemical formula and density, it computes delta and beta. These values of the optical constants are then supplied to IMD which then performs its calculations (i.e. reflectance, transmission, etc.)

## 3. DATA

Here we present the reflectance data measured at ALS Beamline 6.3.2 on June 13-15, 2003. We separate the data presented here into three categories depending upon the grazing incidence angle at 5˚, 10˚, or 15˚. The graphs are split up into the corresponding wavelength scans available at Beamline 6.3.2. These wavelength scans include 2.7-4.8 nm, 4.4-6.8 nm, 6.6-8.8, and 8.4-11.6 nm.



Downloaded From: http://proceedings.spiedigitallibrary.org/ on 03/19/2014 Terms of Use: http://spiedl.org/terms

### 3.1 Reflectance Comparison at 5˚

Note that each chart has three lines. The curves with squares, circles and triangles correspond to the measured reflectance of UOx, NiO on Ni, and Ni on Quartz respectively. This is what these labels mean:

1. UOx stands for uranium with its native oxide which is almost $UO_2$.
2. NiO on Ni stands for evaporated Ni on a Silicon wafer. We brought a deep UV/ ozone lamp to the ALS for the purpose of cleaning the adventitious carbon-containing layer off our samples. This lamp is known to remove the "organic layer" from the native oxide coating a silicon wafer in about 45 seconds.[18] (This can be seen on silicon surfaces which go from hydrophobic to hydrophilic in about 45 seconds as the carbon containing layer on top dissipates). To insure that the sample had an ample opportunity to lose organic materials we exposed our nickel to three full minutes of UV light. However, the most obvious change was not the elimination of carbon but the darkening of the surface. We take this coloring to be tarnishing (oxidation) of the metal. This oxidation needs to be further investigated to see if the darkening is due to oxidation and what thickness of oxide is produced.
3. Ni on Quartz- This sample wasn't cleaned with UV light. Its surface remained visibly bright. However, the usual surface quality of the quartz is not as high as is typical for the silicon wafers. One of the evidences is in the figure error seen for the nickel on quartz sample. It wasn't flat. At ALS, when we sought to align the sample at low angles we could see the image of the soft x-ray beam smeared out or broken up into several bands depending on the spot on the sample which it illuminated. In contrast, the reflected image off of the nickel-on-silicon-wafer sample focused well. We had previously measured via AFM the surface roughness of silicon wafers and quartz samples with and without coatings. We have always observed the surface smoothness of our quartz sample to be inferior to those of silicon. We had not measured the nanoroughness of the nickel coated quartz sample but speculate that it is rougher than the silicon samples.

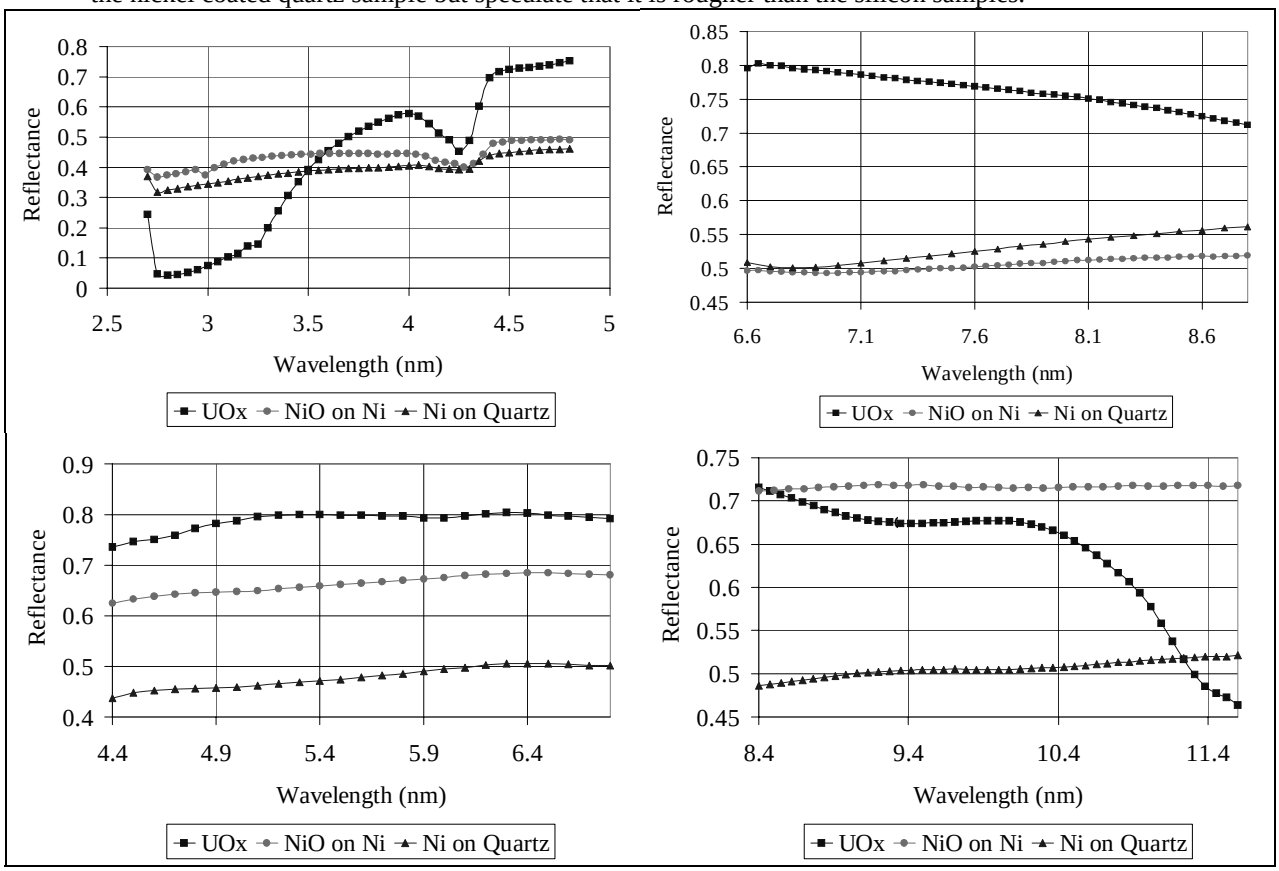



**Fig. 4: Measured reflectance of UOx, NiO on Ni, and Ni on quartz at 5˚ from 2.7 to 11.6 nm.**



Downloaded From: http://proceedings.spiedigitallibrary.org/ on 03/19/2014 Terms of Use: http://spiedl.org/terms

As shown in Fig. 4, at 5˚ uranium oxide reflects more than nickel from 3.6 to 8.5 nm. At this lower grazing incidence angle, uranium oxide has a maximum reflectance of 80% from 5.2 to 6.6 nm as shown in Fig. 4. This value is 20-40% greater than the reflectance of nickel here. Notice in Fig. 4 the dip in reflectance of all three graphs at about 4.3 nm. This may corresponds to the absorption edge of carbon near 4.3 nm (about 284 eV)[10] which may be due to thin organic layers that form on surfaces when they are exposed to ambient air.[18] In Fig. 4, we also notice two interesting features of uranium oxide. First, we notice a feature similar to an interference minimum at about 9.4 nm which we will see appear more strongly at higher angles. Second, we notice an apparent absorption edge at 11.4 nm.

### 3.2 Reflectance Comparison at 10˚

The next four figures show the reflectance comparisons of uranium to nickel at 10˚ grazing incidence. First, notice once again that an absorption edge appears near 4.3 nm. The reflectance of this uranium sample exceeds that of nickel at 5.5 nm and continues at nearly double the reflectance of nickel over most of this range until at 10.5 nm it falls below the reflectance of our Ni film. By closer examination, discrepancies in the reflectance from one wavelength range to the other can be observed. As stated earlier, this may be an artifact of the use of different filters at different wavelengths from Beamline 6.3.2. Also, we notice in Fig. 5 once again that uranium's absorption edge does not appear at 11.1 nm. Furthermore, we see more pronounced the presence of a minimum in uranium oxide's reflectance at 10 nm.

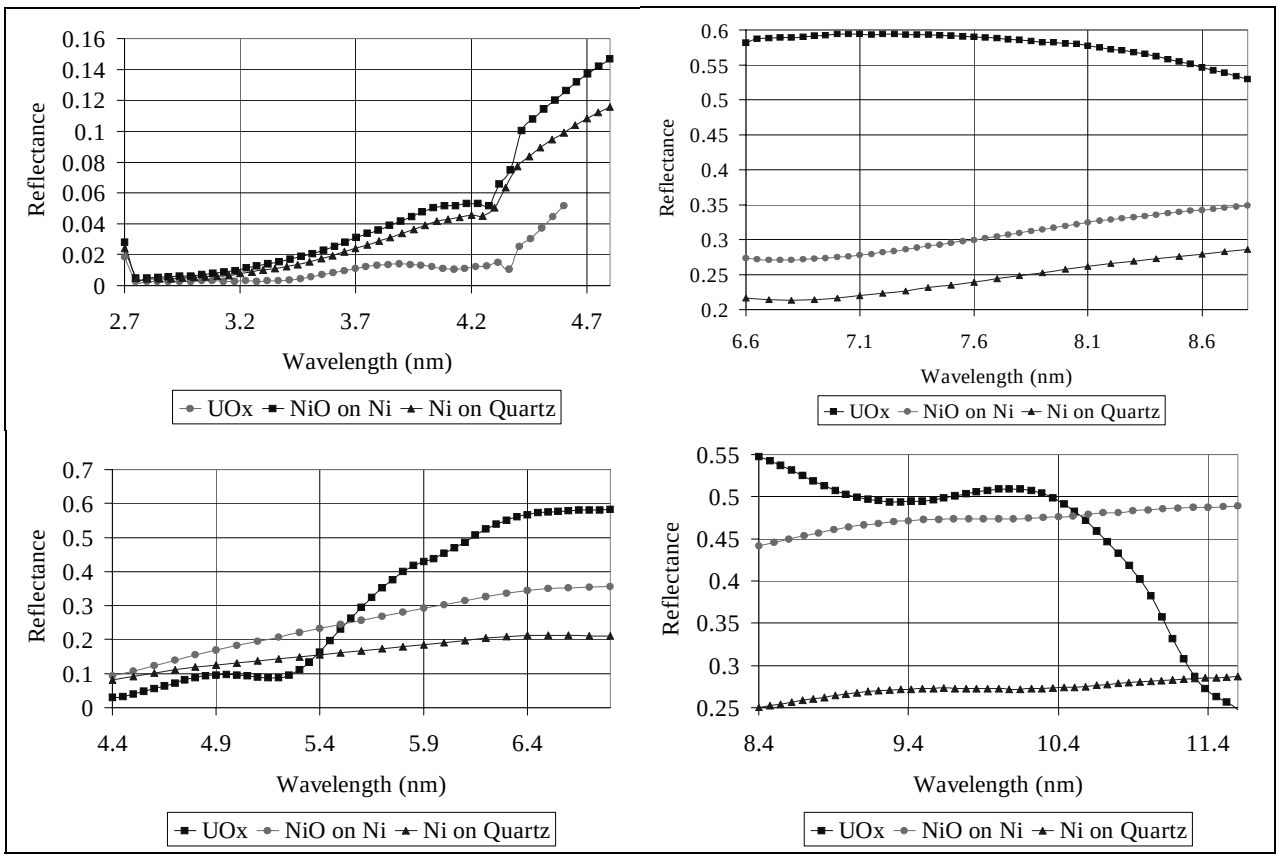



**Fig. 5: Measured reflectance at 10˚ of UO2, NiO on Ni, Ni on Quartz from 2.7-11.6 nm.**



Downloaded From: http://proceedings.spiedigitallibrary.org/ on 03/19/2014 Terms of Use: http://spiedl.org/terms

### 3.3 Reflectance Comparison at 15˚

At 15˚, uranium oxide reflects more than nickel from 6.3 nm to 10.9 nm. As seen in Fig. 6, uranium oxide reaches a maximum reflectance of 33% at 10.3 nm. This wavelength also corresponds to a strong interference fringe. The existence and significance of this fringe will be discussed in section 4.2.

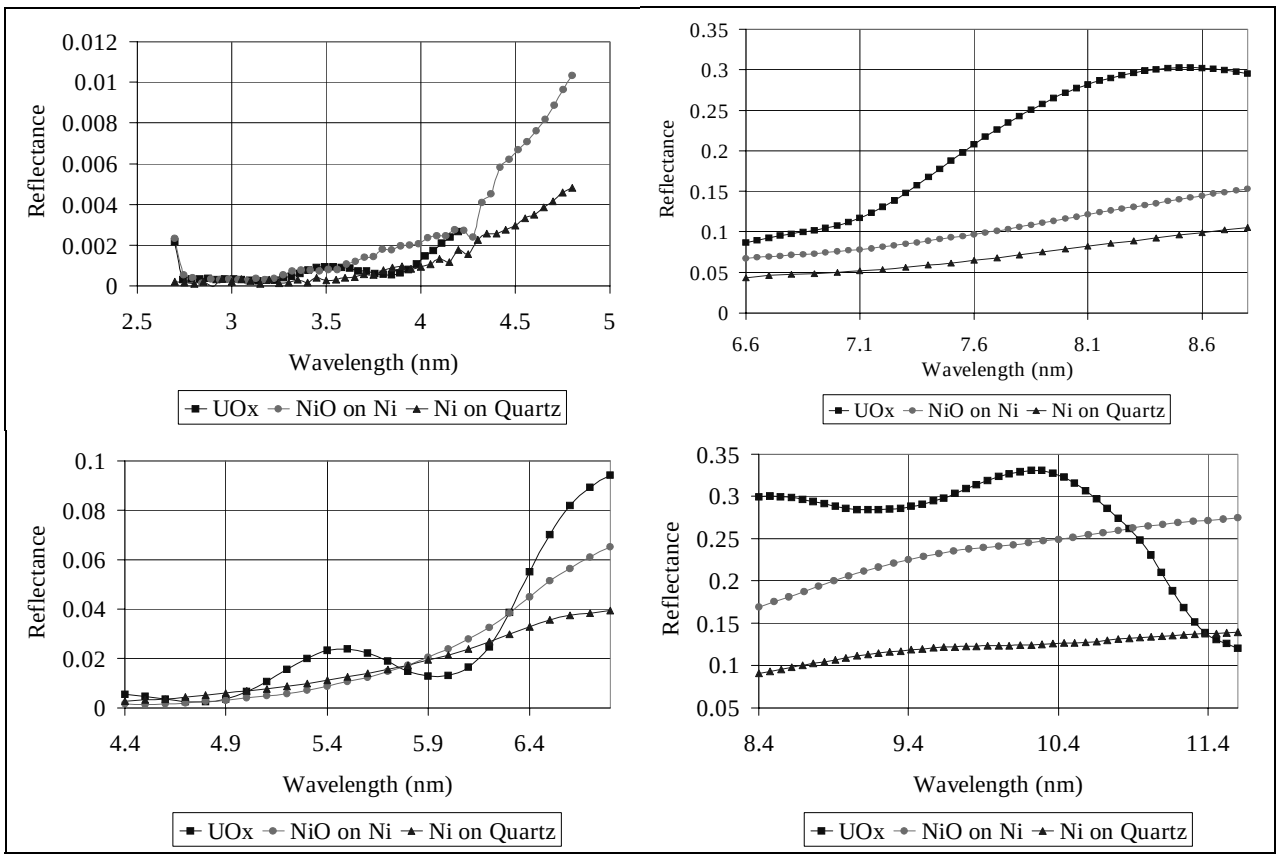



**Fig. 6: Measured reflectance at 15˚ of UO2, NiO on Ni, and UOx from 2.7 to 11 nm.**

## 4. DISCUSSION OF RESULTS

### 4.1 Naturally oxidized uranium is a better low-angle reflector than nickel

As shown in the previous figures, uranium oxide single-layer thin films reflect more than nickel films from about 5-10 nm in agreement with modeled calculations. At 5˚ grazing incidence, uranium oxide reflects more than nickel or nickel oxide from 3.5-8.4 nm. At 10˚, uranium oxide reflects more than nickel or nickel oxide from 5.5-10.5 nm. And at 15˚, uranium oxide reflects more than the nickel samples from 6.3-10.9 nm. Notice that uranium oxide has a very high reflectance over these wavelengths as predicted by computed reflectance, especially at higher grazing incidence angle. This makes uranium oxide ideal for low angle single-layer reflectors for synchrotron, astronomical, and other optics applications in the soft x-ray and EUV region. We strongly recommend further development and application for uranium oxide as a thin film for these applications as they have already proved themselves in previous astronomical applications.[3,5]



Downloaded From: http://proceedings.spiedigitallibrary.org/ on 03/19/2014 Terms of Use: http://spiedl.org/terms

### 4.2 Comparison to atomic scattering factor model with CXRO/IMD

In this section we strive to understand further how the different aspects of our samples (composition, density, thickness, and roughness) affect their reflectances. In the CXRO website and IMD, we prepared layer structures with composition, density, layer thickness and roughness which correspond to the measured layer thickness of our samples. We used handbook densities,[10] published chemical compounds for the oxidation states and composition[19,20], approximate layer thicknesses taken from XRD and deposition rates, and estimated roughness. Using those computer programs we computed our structures' reflectances and compared them to the measured reflectances. Below we show an analysis using the CXRO webpage to compute the reflectances of various structures similar to what we think the $UO_x$ sample has. Additionally, we compare the 2.1 to 6.0 nm reflectance of the three measured samples ($UO_x$, NiO on Ni, and Ni on quartz) to computed reflectances from similar layer structures in IMD (Fig. 9-10).

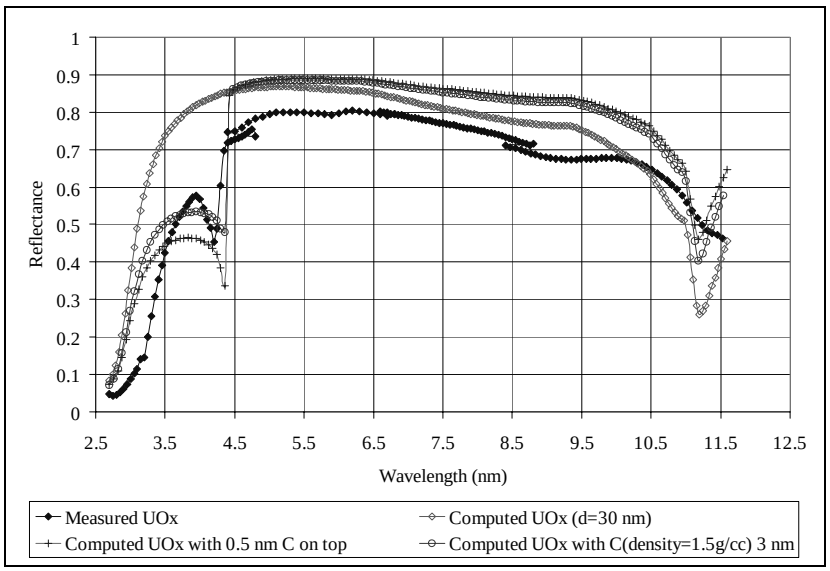



**Fig. 7: Reflectances at 5˚ of measured $UO_x$ and three structures modeled from the CXRO website. The three structures models are 30 nm of $UO_2$ with no carbon contamination on top, 30 nm of $UO_2$ with 0. 5 nm of carbon on top, and 30 nm of $UO_2$ with 3 nm of carbon contamination on top (density=1.5 g/cc). Notice how the absorption edge predicted by the atomic scattering factor model used in the CXRO models does not appear in the measured data.**

Fig. 7 contains a composite graph for the measured reflectance at 5° for the uranium oxide sample from 2.5 to 11.5 nm. Also plotted are the computed reflectances of three structures similar to the actual uranium oxide film which we chose to try to match the experimental data. The single-layer and bilayer options at the CXRO website were employed to obtain these plots. The values of the optical constants for compounds at CXRO are computed using the ASF model.

There are four features in the uranium oxide reflectance curve shown in Fig. 7 which merit comment. We focus first on the pronounced dip in the reflectance at about 4.3 nm. If the reflectance were that of $UO_2$ as given by the ASF model then the surface would reflect about 86% rather than the measured 50%. Additionally, the lower reflectance persists for all reflectances below 4.3 nm. This appears to be an absorption edge. We believe it could be the absorption edge of carbon—probably organic carbon. Previous XPS studies on samples prepared in the same manner as these have revealed small amounts of carbon on or near the surface. Ellipsometry has given approximate values of this carbon containing contamination layer to be <2 nm.[18] Two of the curves in Fig. 7 were computed for models where we had put an ultra-thin film of carbon on the uranium oxide. There are several difficulties with this interpretation. The shape of the curves below the minimum does not match the observed decrease. The observed peak is narrower. Furthermore, the reflectance of the uranium falls off much quicker than predicted. Another difficulty with this interpretation is that the bottom of the dip is about 0.2 nm lower (8 eV higher) than where the computed dip should be for a carbon-containing top layer. This might suggest that the minimum is due to an edge in $UO_2$ except that the same dip, with the same



Downloaded From: http://proceedings.spiedigitallibrary.org/ on 03/19/2014 Terms of Use: http://spiedl.org/terms

displacement is seen in the Ni samples (Fig. 9-10). The minima of the carbon absorption trough for all three measured reflectances are located near 42.5 nm as compared to IMD's predicted locations near 43.7 nm. Additionally, NiO on Ni and Ni on quartz samples have nearly identical reflectance minima at 3.0 nm. Perhaps this feature could suggest the presence of nitrogen on their surfaces. Why is there a 0.2 nm shift? We do not know. Some of the reflectance features discussed here, perhaps even most, could be chemical bonding effects. It would be profitable to refer to XPS to see the kinds and magnitudes of shifts seen in carbon containing materials. The ASF model ignores chemical bonds completely. (See discussion in section 2.4).

This merited further study so we calculated the reflectance of a model system to understand it. We chose the following structures. For the $UO_x$ we chose 31.8 nm of uranium dioxide ($UO_2$) with 3.75 nm of a layer of polycarbonate on top. It is the organic in the IMD data base which we thought is best representative of the organic material which settles on most surfaces.[18] The form we used is lexan ($C_{10}H_8O_4$). Fig. 8 compares the measured reflectance of $UO_x$ with the IMD computation using this model.

Fig. 9 and Fig. 10 show the measured reflectance for NiO on Ni and Ni on quartz respectively with their corresponding IMD-computed reflectances. From XRD, we found that the apparent Ni thickness was 49.7 nm. We expected to have some oxidation on the surface as well as carbon contamination. For the NiO on Ni structure, we found that 2.0 nm of NiO on top of a variable thickness of Ni with 2.0 nm of carbon contamination and 2.0 nm of surface roughness gave us the best fit. A variable thickness of the Ni layer came from the fact that after the original 2.0 nm of NiO with 10.0 nm of Ni underneath, any additional thickness of Ni did not change our computed reflectance. This would leave us to believe that 2.0 nm of NiO with 10.0 nm of Ni underneath would be opaque in this wavelength region. The Ni on quartz structure had 2.0 nm of NiO on top of a variable thickness layer of Ni on a quartz substrate. The NiO layer had 2.0 nm of polycarbonate carbon contamination on top and 5.2 nm of surface roughness. This roughness is assumed to be due to the unpolished nature of the quartz substrate.

The curves also show that the magnitude of this dip can arise from very little carbon in or on the sample. As little as 0.5 nm of graphite could do this. Graphite, however, is not a possible contamination layer. A more likely source of this carbon contamination layer is a naturally occurring hydrocarbon, such as an oil, which is deposited on the sample from the ambient air. The shape of the absorption band on the low wavelength (high energy) side of the measured data is especially different. This brings us to the second discrepancy.

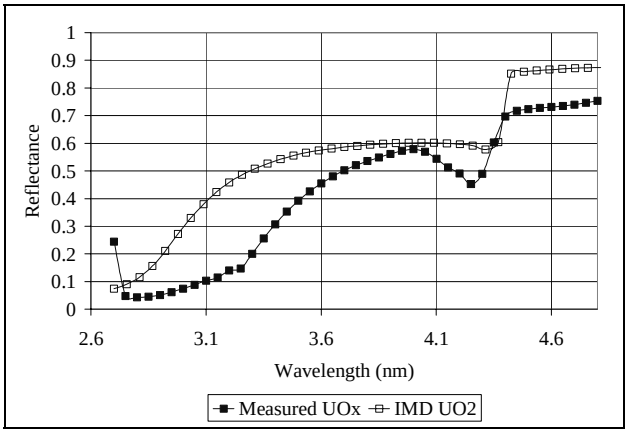



**Fig. 8: Measured $UO_x$ and IMD computed reflectances (at 5˚). The computed structure was modeled as 31.8 nm of $UO_2$ on top of silicon with 3.75 nm of carbon contamination on top.**

We return now to the features in the uranium oxide reflectance curve shown in Fig. 7 which merit comment. The second issue is the overall shape and magnitude of the curve. If one does not look at details, the four curves in Fig. 7 are rather similar. They indicate that $UO_2$ should have low reflectance at either end of the interval of interest, especially the low wavelength (high energy) end. But the details are significantly different. The computed curves generally are higher



Downloaded From: http://proceedings.spiedigitallibrary.org/ on 03/19/2014 Terms of Use: http://spiedl.org/terms

than the measured data, about 10 percentage points higher in the middle of the range, but much larger at the low wavelength end.

There is an absorption edge predicted in uranium metal at about 11.2 nm. At this point the reflectances of all of the computed curves show a deep and pronounced dip. This is not seen in the ALS measured data. Instead there is a gradual decline. No amount of work with the given atomic scattering factors can model this feature in the experimental data. The optical constants of the oxide will have to be determined independently. In fact, Shannon Lunt has done so for a related material, reactively sputtered $UO_x$.[7]

Lastly there is broad minimum in the reflectance of the measured uranium at about 9 nm. This is followed by a maximum at about 10 nm. This is even more clearly seen in the measured data at 10 and 15 degrees (see Figs. 5 and 6). In contrast to this form the computed reflectance is linear.

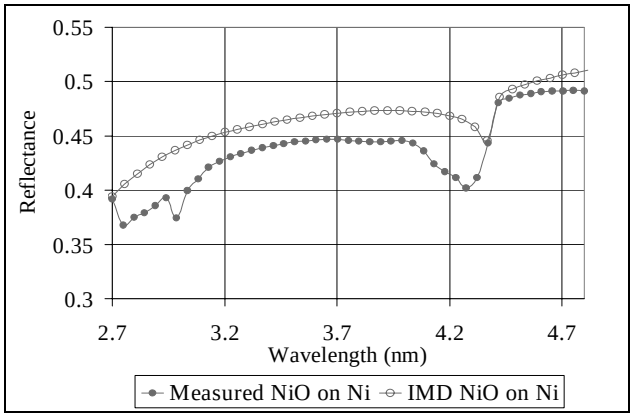



**Fig. 9: Measured NiO on Ni and IMD computed reflectances (at 5˚). The computed structure was modeled as 2.0 nm of NiO on top of 47.7 nm of Ni on a silicon substrate with 2.0 nm of surface roughness and 2.0 nm of carbon contamination.**

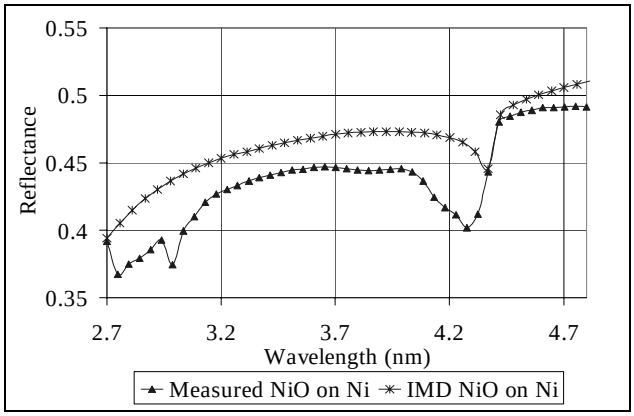



**Fig. 10: Measured Ni on quartz and IMD computed reflectance (at 5˚). The computed structure was model as 2.0 nm of NiO on top of 47.7 nm of Ni on a quartz substrate with 5.2 nm of surface roughness and 2.0 nm of carbon contamination**

## 5. CONCLUSIONS

Naturally oxidized uranium thin-film reflectors were found to be more reflective than nickel or nickel oxide on nickel over a large range of angles and wavelengths as predicted by the ASF model. Specifically, uranium oxide reflects more than nickel at 5˚ grazing incidence from 4.5 to 8.5 nm, at 10˚ from 5.5 to 10.5 nm, and at 15˚ grazing incidence from 6.2 to 10.9 nm. The maximum reflectance from 2.7 to 11.6 nm of this uranium oxide was measured to be an impressive 80% at 5˚, 60% at 10˚, and 30% at 15˚ grazing incidence. We therefore recommend that uranium oxide-based mirror coatings should be developed and implemented for future projects where broadband, low angle, soft x-ray mirrors are required. We additionally report that nickel-oxide coatings reflect more than nickel at lower wavelengths (higher energies). The oxidation rate and oxidation process of nickel are currently being investigated and will be reported in a future article. Another finding of this report is that the complex indices of refraction probably differ noticeably from the reported values from the atomic scattering factor model at the higher wavelengths. We conclude this based upon inability of the ASF model to reproduce the (interference fringe) minimum at about 9.5 nm in the ASF model and by the fact that the absorption edge is not at 11.1 nm as reported by the model. We suggest that the absorption or $\beta$ is less than the ASF model predicts for $UO_2$. We are in the processes of determining the index of refraction for naturally oxidized uranium over the soft x-ray and EUV range.



Downloaded From: http://proceedings.spiedigitallibrary.org/ on 03/19/2014 Terms of Use: http://spiedl.org/terms

## ACKNOWLEDGEMENTS

We are grateful to Hollilyn Drury and Megan Rowberry for aiding in sputtering the uranium film studied. An SPIE scholarship to Richard Sandberg and BYU Department of Physics and Astronomy research funds aided in the research. We also acknowledge grateful the financial contributions of V. Dean and Alice J. Allred and Marathon Oil Company (US Steel) for gifts to Brigham Young University for thin-film research. We thank all the members of the BYU EUV team for their support. We are grateful to Eric Gullikson and Andy Aquila at ALS Beamline 6.3.2 at LBNL for their help in data interpretation, reduction, and analysis.

## REFERENCES

[1] David D. Allred, Matthew B. Squires, R. Steven Turley, Webster Cash, and Ann Shipley, "Highly Reflective Uranium Mirrors for Astrophysics Applications," in *X-ray Mirrors, Crystals and Multilayers*, Andreas K. Freund, Albert T. Macrander, Tetsuya Ishikawa, and James. T. Wood, Editors, Proc. SPIE **4782**, pp. 212-223, SPIE, Bellingham, WA, 2002.

[2] Webster Cash, Private Communication.

[3] See, for example, a. D.D. Allred, R. S. Turley, and M. B. Squires, "Dual-function EUV multilayer mirrors for the IMAGE mission," in EUV, X-Ray and Neutron Optics, Carolyn A. Macdonald, Kenneth A. Goldberg, Juan R. Maldonado, H. Heather Chen-Mayer, and Stephen P. Vernon, Editors, Proceedings of SPIE 3767, pp.280-287, SPIE, Bellingham, WA, 1999.
b. Matthew B. Squires. The EUV Optical Constants of Sputtered U and a-Si, Honors Thesis, Brigham Young University, Provo, UT, April 1999. http://volta.byu.edu

[4] Hans Pew, Private Communication.

[5] B. R. Sandel, A. L. Broadfoot, J. Chen, C. C. Curtis, R. A. King, T. C. Stone, R. H. Hill, J. Chen, O. H. W. Sigmund, R. Raffanti, David D. Allred, R. Steven Turley, D. L. Gallagher, "The Extreme Ultraviolet Imager Investigation for the IMAGE Mission," Space Science Reviews 91, pp. 197-242 (2000).

[6] David Oliphant (oliphantd@byui.edu), *Characterization of Uranium, Uranium Oxide and Silicon Multilayer Films*, Masters thesis, Dept. of Physics and Astronomy, BYU, Provo, UT 2000. Contact the BYU HBL library at http://www.lib.byu.edu/hbll/ or in partial form at http://www.byui.edu/Ricks/employee/oliphantd/ .

[7] The curves for these plots were computed at the CXRO website http://www-cxro.lbl.gov/optical_constants/mirror2.html (June-July, 2003) using the option "thick mirrors", that is, single surface mirrors with zero surface roughness. The refractive indices, which are needed for the calculation, were calculated using the atomic scattering factor model using densities which we supplied the program. We used the CRC Handbook of Chemistry and Physics for densities. That is, there was no effort made to obtain the actual densities of the films. Densities: David R. Lide, Ed., CRC Handbook of Chemistry and Physics, 71st edition, CRC Press, Boca Raton, 1990-91

[8] Shannon Lunt, *Determining the Indices of Refraction of Reactively Sputtered Uranium Dioxide Thing Films from 46 to 584 Angstroms*, Masters Thesis, Dept. of Physics and Astronomy, BYU, Provo, UT 2002. Contact the BYU HBL library at http://www.lib.byu.edu/hbll/

[9] G.B Thompson and D.D. Allred, "Reactive Gas Magnetron Sputtering of Lithium Hydride and Lithium Fluoride Thin Films," J.X-ray Sci. Technol. 7, pp. 157-170, 1997.

[10] David R. Lide, Ed., CRC Handbook of Chemistry and Physics, 71st edition, p.10-256, CRC Press, Boca Raton, 1990-91.

[11] Kristi R. Adamson, to be published in Utah Academy of Arts and Sciences.

[12] Hollilyn Drury and Megan Rowberry, May 2003 International Science Fair, Columbus OH, USA.

[13] Program for EUV and X-ray reflectance calculations, courtesy of Prof. David L. Windt: windt@astro.columbia.edu. http://cletus.phys.columbia.edu/windt/idl .

[14] J.H. Underwood *et al*. "Calibration and standards Beamline 6.3.2 at the Advanced Light Source." Rev. Sci. Instrum., 67 (9), 1-5 (1996).

[15] http://www-cxro.lbl.gov/als6.3.2/, July, 2003 or contact Eric Gullikson from the webpage for additional questions.

[16] CXRO webpage (July, 2003). http://www-cxro.lbl.gov/optical_constants/intro.html.

[17] B.L. Henke, E.M. Gullikson, and J.C. Davis, *X-ray interactions: photoabsorption, scattering, transmission, and reflection at E=50-30000 eV, Z=1-92*, Atomic Data and Nuclear Data Tables **54** no.2, 181-342 (July 1993).

[18] A thorough investigation of this carbon contamination and methods for preventing and cleaning contamination will be submitted soon in the Journal of Vacuum Science and Technology.

[19] B. W. Veal and D. J. Lam, "X-ray photoelectron studies of thorium, uranium, and their dioxides." Physical Review B, 10 (12), 902-8 (1974).

[20] R. J. Thorn, "Intensities and Satellites of 4f-photoelectrons in Thorium and Uranium Dioxides." J. Phys. Chem. Solids, 43 (6), 571-5 (1982).



Downloaded From: http://proceedings.spiedigitallibrary.org/ on 03/19/2014 Terms of Use: http://spiedl.org/terms